ELSEVIER

Journal of Alloys and Compounds 444–445 (2007) 345–351

Journal of ALLOYS AND COMPOUNDS

www.elsevier.com/locate/jallcom

Uranium and U–Zr and U–Ru alloy corrosion rates in the transpassive state

A. Maslennikov [a], A. Bessonov [a], V. Peretroukhine [a,*], N. Budanova [a], K. Gedgovd [a], G. Bulatov [a], A. Tsivadze [a], C. Delegard [b]

[a] *Institute of Physical Chemistry and Electrochemistry, Russian Academy of Sciences, 31 Leninsky Prospect, Moscow 119991, Russia*

[b] *Pacific Northwest National Laboratory, P.O. Box 999, Richland, WA 99352, USA*

Received 12 December 2006; received in revised form 20 June 2007; accepted 20 June 2007
Available online 29 June 2007

Abstract

Electrochemical studies of reactor-grade uranium metal and its alloys with Zr and Ru in neutral electrolyte (0.1 M $NaClO_4$, pH 3.0–9.0) in the potential region close to uranium's transpassivation threshold were performed. Transpassivation potentials from 320 mV/Ag/AgCl (U–1.3 at.% Zr) to 470 mV (U–10.5 at.% Ru) were found to be weakly affected by added alloying element concentration and electrolyte pH. Comparison of *I–t* curves registered on U metal, U–1.3 at.% Zr, and –1.2 at.% Ru electrodes indicate that the electrochemical oxidation rate of alloyed uranium was lower than that of pure U metal. The difference of the electrochemical oxidation rates was dependent on electrolyte pH. The calculated corrosion rates of uranium metal and alloy increased from 0.89 mg cm^{-2} h^{-1} (U–1.3 at.% Zr, $E = 300$ mV/Ag/AgCl) to 40.4 mg cm^{-2} h^{-1} (U metal, $E = 600$ mV/Ag/AgCl) and were found to be independent of alloy addition and electrolyte pH. The contribution of spallation of non-oxidized uranium species from the electrode surface to the observed corrosion rates was made.

Keywords: Uranium; Alloys; Corrosion; Electrochemical

1. Introduction

Numerous studies of uranium metal and uranium alloy corrosion in water and aqueous solutions, carried out since the 1940s [1–3], show that hydrated uranium dioxide $UO_{2+x}{\cdot}nH_2O$ ($x < 0.3$) is the principal reaction product. Apparently, the formation of UO_{2+x} includes the primary oxidation of uranium metal to U(III) as an intermediate product. However, due to the low stability of U(III) ions towards oxidation in aqueous solutions [4,5], its steady-state concentration during uranium corrosion is negligible and cannot be proved experimentally. Data on the kinetics of uranium metal and alloys corrosion, summarized in [6], were obtained using weight gain (WG) or metal loss (ML) techniques. Corrosion tests with duration from 100–200 to 2000 h reveal that sometimes the uranium metal oxidation starts with an induction period, lasting from 10 to 200 h, followed by the reaction of zero order versus metal mass loss. The Arrhenius plots collected in [6] can be used to estimate the reactor-grade uranium metal corrosion rate at room temperature (20 °C) to be 0.005–0.025 mg cm^{-2} h^{-1}. Estimates of uranium metal corrosion rate, using a published empirical equation [7] to account for the effects of pH and complexing agents, yields values ranging from 0.5 to 0.7 μg cm^{-2} h^{-1}, corresponding to the increase of the electrolyte pH from 5.0 to 9.0, contradicting the estimates using the equation presented in [6]. Determination of uranium metal corrosion rates using the quantitative determination of H_2 formed during a fixed period of time [8,9] results in rates consistent with those obtained by WG or ML techniques.

Doping of uranium with other metals increases its corrosion resistance if the alloy addition stabilizes uranium's γ-phase at the required temperature [6]. In a few published reviews [1,2,6,10–13], the effects on the uranium alloys' corrosion rates in water were studied for Mo, Zr, and Nb, all known to stabilize γ-U at room temperature. It has been stated that alloy additions below threshold concentrations have no statistically significant effect on the alloy corrosion rate in comparison with

* Corresponding author. Tel.: +7 495 333 85 22; fax: +7 495 335 17 78.
E-mail address: vperet@ipc.rssi.ru (V. Peretroukhine).

0925-8388/$ – see front matter © 2007 Published by Elsevier B.V.
doi:10.1016/j.jallcom.2007.06.078

pure uranium metal. The threshold alloy addition concentrations (>8 at.% Mo [2,11], >20 at.% Zr [14] and >4 at.% Nb [15]) were determined. Alloy addition to concentrations exceeding the threshold concentration decreases the alloy corrosion rate 100–1000-times compared with the rate for reactor-grade uranium metal. At the same time, no quantitative regularities associating the alloy addition concentration with the observed values of corrosion rates are revealed.

The extensive studies of the electrochemical behavior of uranium metal and its alloys with Zr, Mo, and Nb in aqueous solutions demonstrate that hydrated UO_{2+x} ($x < 0.1$) forms a passive film at the electrode surface at oxidation potentials from −500 to 500 mV/SCE [3,16,17]. Shifting the oxidation potential towards more positive values transfer the uranium metal electrode to the transpassive state, characterized by the transpassivation potential ($E_{tr.}$), at which UO_{2+x} oxidizes to U(VI) species whose solubility is determined by the electrolyte acidity.

The composition of corrosion products formed by 30-year storage of 115,000 Al-clad and, primarily, Zr-clad U metal fuel elements (2100 tonnes) in water-cooled K East and West fuel storage basins (US Department of Energy Hanford Site) [9,18] differed from those expected in light of fundamental corrosion studies of reactor-grade uranium metal and its binary alloys [1,2,6]. The presence of uranium hydride (UH_3) and U(VI) compounds, including U(VI) peroxide ($UO_4{\cdot}2H_2O$), in the product sludge was demonstrated by XRD analysis [16]. The presence of U(VI) in different chemical forms in the sludge may indicate that the oxidation potential at the uranium fuel rod–water interface in K basins may be close to $E_{tr.}$. Alternatively, it may indicate the oxidation of UO_2 occurred in later reactions, for example with dissolved oxygen or by H_2O_2, generated at U metal–aqueous solution interface due to the radiolytic effects. The higher oxidation potential may arise from galvanic corrosion couples, including with the cladding (especially Al), from fission product accumulation in the irradiated uranium, or radiolytic effects providing high steady-state H_2O_2 concentrations at the U metal–electrolyte interface as has been observed for UO_2 electrodes [19].

The present study, being a part of fundamental investigations of the effect of different factors on uranium behavior in the K basins, is directed to determine the effects of small alloy additions on the corrosion rates of irradiated uranium metal in contact with water in the range of potentials close to uranium metal transpassivation. Linear voltammetry (LV) and potential controlled electrolysis (PCE) were chosen as the principal measurement techniques for the study. Because any corrosion process involves heterogeneous electron transfer and ion diffusion, electrochemical techniques provide better quantitative data compared with non-electrochemical techniques [16].

2. Experimental

2.1. Uranium metal and alloy sample preparation and characterization

Uranium metal of reactor-grade purity was prepared using the conventional technique of UF_4 reduction with Ca metal in vacuum at 1600 °C. The impure metal reduction product was refined in vacuum using graphite crucibles with MgO-coated inner surfaces to avoid UC contamination of refined U metal. Impurity concentrations in the refined metal varied from 0.02 ppm (B) to 0.6 ppm (Fe, Al) and correspond to the purity of reactor-grade uranium [20]. The vacuum-refined uranium samples then were rolled and drawn to give the rods with ∅ = 2-mm cross-sectional diameter and 15-mm length. Final annealing of the rods in vacuum at 1073 K for 2 h stabilized α-uranium metal with the grain size and microhardness as shown in Table 1.

The U metal and 99.7 wt.% purity Zr and Ru metals were used as starting materials to produce U–1.3 at.% Zr, U–5.0 at.% Zr, U–1.2 at.% Ru, and U–10.5 at.% Ru alloys. The alloys were prepared by arc-melting in water-cooled copper crucibles with an inert non-consumable tungsten electrode. The arc-melting procedure was conducted three times with high purity Ar purge of the furnace volume and intermediate evacuation to 5×10^{-3} Torr residual pressure. The working Ar pressure in the reactor while melting was 150–200 Torr. The sample melting was repeated three to four times to improve alloy homogeneity. Rough alloys were annealed at 1230 K for 24 h at 5×10^{-5} Torr to further improve the alloy homogeneity. The ingots were rolled to 5.5-mm diameter at 880–900 K to maintain the uranium alloy in the alpha phase. The electrodes for the corrosion tests were turned mechanically to 4-mm diameter and annealed at 1073 K at 5×10^{-5} Torr for 2 h to relieve stresses from the mechanical treatment.

The electrodes for the corrosion tests were fabricated by placing the prepared rods into the tightly fitting Teflon tips of a conventional rotating disk electrode. The electrodes were polished mechanically with abrasive papers to a 0.5-μm finish or electrochemically in a CH_3COOH–CrO_3 bath, rinsed with distilled water and acetone, and stored under high purity Ar.

2.2. Reagents

All electrolytes used in the present study were prepared using analytical grade $NaClO_4$ and distilled water. Electrolyte pH was adjusted by the addition of 0.01 M $HClO_4$ or 0.01 M NaOH analytical grade arsenazo III and HCl were used as received for the quantitative determination of U(VI).

2.3. Electrochemical tests

The three-electrode electrochemical measurement system was comprised of a uranium-rotating disk working electrode (EDI101T Radiometer), Ag/AgCl reference electrode (Radiometer), and a 0.3-mm diameter Pt wire auxiliary electrode. A 10-ml volume Pyrex electrochemical cell was used in all tests.

Table 1
Phase composition, microstructure and microhardness of uranium metal and alloys

Alloy	U/Me ratio	Phase composition		Crystallite size (μm)	Microhardness (kg mm^{-2})	Microhardness (kg mm^{-2}), data from [24]	
		XRD	SEM			Alloy	Value
U metal	–	α-U	α-U	250–300	160 ± 5	U metal	160–170
U–1.3 at.% Zr	76 ± 15	α-U	α-U	200–250	326 ± 16	–	–
U–5.0 at. % Zr	189 ± 12	α-U	α-U ± δ	60–80	346 ± 13	U–5 at.% Zr	340–350
U–1.2 at.% Ru	–	α-U	α-U ± U_2Ru	50–70	375 ± 10	U–5.0 at. Ru	400–553
U–10.5 at.% Ru	–	α-U	α-U ± U_2Ru	10–40[a]	555 ± 11	U–7.5 at. Ru	400–615

[a] Crystallite U_2Ru (Fig. 1C).

The cell was attached to a MDE150 electrochemical stand (Radiometer), which also provided an inert-gas (high purity Ar) purge and communication with the potentiostat. A digital electrochemical analyzer (DEA332, Radiometer) operated under Voltamaster-2 software (Radiometer) was used to acquire the electrochemical data. The linear voltammetry (LV) technique was used to determine the transpassivation potentials of the U metal and alloys. Corrosion rates were determined using the potential controlled electrolysis (PCE) technique.

3. Results and discussion

3.1. Characterization of uranium metal and alloy samples for electrochemical corrosion tests

Phase composition, SEM data, including crystallite size, and microhardness of the prepared uranium metal and alloy samples are shown in Table 1. As expected, by the applied experimental procedure, the XRD analysis demonstrated that the uranium metal and alloys were in the α-phase. The metal crystallite size 250–300 μm was determined from the corresponding microphotograph (Fig. 1A).

The chemical compositions of the prepared U–Zr and U–Ru alloys were determined by the quantitative determination of U, Zr, and Ru using ICP AAS (inductively coupled plasma atomic absorption spectroscopy) after dissolution of weighed alloy samples in 14.0 M HNO_3 + 0.01 M HF (U–Zr) [21] and 14.0 M HNO_3 + 2.0 M HCl (U–Ru) [22]. The homogeneity of the prepared U–Zr alloys was determined using SEM and EDX (scanning electron microscopy with energy dispersive X-ray spectrometry). The ratio of intensities of the L_U and K_{Zr} lines were measured in 10 randomly chosen points at the sample surface and found to correspond to U/Zr atomic ratios of 76 ± 1.3 and 18.9 ± 1.2 (corresponding to 5.0 ± 0.1 and 10.5 ± 0.3 at.% Zr).

X-ray diffraction analysis of U–1.3 at.% Zr and U–5.0 at.% Zr alloy samples annealed at 1073 K for 2 h and cooled under quasi-reversible conditions indicated the presence of only α-U phase in the sample (Table 1). At the same time, according to U–Zr thermodynamic data, the solubility of Zr in α-U at 935 K does not exceed 0.05 wt.%. The reversible cooling of U–Zr solid solutions to temperatures below 873 K should form some δ-phase corresponding to the saturated Zr solid solution in α-U. The absence of the δ-phase at the recorded U–Zr alloy diffractogram is due to insufficient sensitivity of the XRD measurements.

The microstructures of the U–1.3 at.% Zr and U–5.0 at.% Zr alloys samples were determined after electrochemical etching in the acetic acid–CrO_3 bath. The microphotograph of the alloy shows polyhedric crystallites with a 60–80 mm grain size. Thus, the addition of Zr to the uranium metal decreased the crystallite size from 300 to 60 μm (Fig. 1B and C) as Zr concentration increased to 5.0 at.% (Table 1). Results of microhardness measurements of U–5.0 at.% Zr and U–12.0 at.% Zr are presented in Table 1. Comparison of the observed values with the microhardness of pure uranium metal (160 ± 0.5 kg mm^{-2}) demonstrates that Zr increased the hardness of the uranium metal structure.

The U–1.2 at.% Ru and U–12 at.% Ru alloys are characterized by two crystallite microstructures. Polyhedric particles of U_2Ru, distinctly observed in the corresponding microphotographs (Fig. 1C and D), resemble the microstructures of

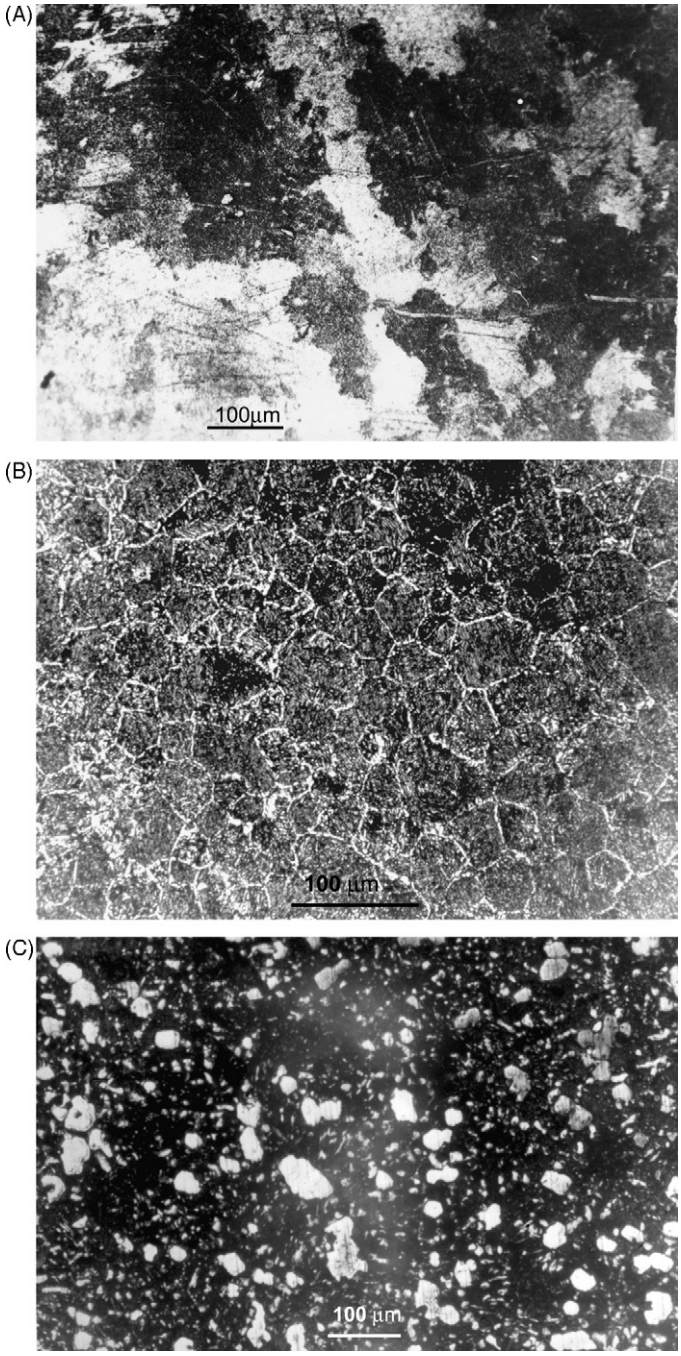

Fig. 1. Surface microphotographs. (A) Reactor-grade uranium metal, (B) U–5.0 at.% Zr alloy and (C) U–10.5 at.% Ru alloy (white spots, U_2Ru).

particles obtained by quenching the U–1 at.% Ru alloy from the γ-phase [23]. The concentration of the U_2Ru particles increased with Ru concentration in the alloy. The microhardness of U–Ru alloys increased with the concentration of alloying metal (Table 1). Apparently, the increased microhardness for the studied alloys indicates that the structural transformation was not accomplished and resulted in formation of δ-phase in the U–Zr alloys and U_2Ru in the U–Ru alloys.

The obtained values of uranium metal and alloys microhardness were compared with the available literature data [24] (Table 1). The comparison demonstrates good coincidence of the

Table 2
Transpassivation potentials of U metal and alloys electrodes in 0.1 M $NaClO_4$ at different pH at a room temperature

pH	U metal $E_{tr.}$ (mV/SCE)	pH	U–1.3 at.% Zr $E_{tr.}$ (mV/SCE)	U–5.0 at.% Zr $E_{tr.}$ (mV/SCE)	pH	U–1.2 at.% Ru $E_{tr.}$ (mV/SCE)	U–10.5 at.% Ru $E_{tr.}$ (mV/SCE)
4.11	463 ± 15	4.05	300 ± 32	419 ± 23	3.04	417 ± 35	410 ± 29
6.02	458 ± 19	6.30	305 ± 29	451 ± 26	5.50	440 ± 28	430 ± 21
6.55	450 ± 12	7.50	310 ± 27	458 ± 19	8.62	442 ± 37	420 ± 32
8.73	445 ± 14	9.00	320 ± 34	465 ± 22	9.77	440 ± 33	336 ± 24

data even for the alloys of similar composition. The insignificant difference observed in the values of U–Ru microhardness may be accounted for the difference in the alloy thermal treatment.

3.2. Linear voltammetry measurements

LV measurements were made on reactor-grade uranium metal electrodes and on the uranium alloy electrodes listed in Table 2. All measurements were performed at ambient temperatures in electrolyte saturated with high purity Ar. Before the start of the measurement, the polished electrode was immersed in the electrolyte and its open circuit potential (OCP), i.e., the electrode potential at zero current, was measured. Within a short time (e.g., about 30 min for pure U metal), the OCP stabilized to ±30–50 mV for the various studied electrodes. After achieving steady state at the electrode surface, the LV measurement started from the OCP value to 1500 mV/Ag/AgCl. All of the obtained curves were of the same form as was observed for the reactor-grade uranium metal shown in Fig. 2. The region characterized by anodic current densities less than 20 μA cm^{-2} that were independent of the applied potential (i.e., the zone of passivity) lasted from the OCP to about 320–450 mV/Ag/AgCl. At the threshold potential marking transition to the transpassive zone, $E_{tr.}$, an increase of the anodic current was observed. The $E_{tr.}$ value was determined as the intersection of the linear extrapolation of ascending part of LV curve with the *x*-axis at zero current density. Data on the uranium metal and alloys transpassivation potentials, and their changes with electrolyte pH, are gathered in Table 2. The data indicate that low concentrations of

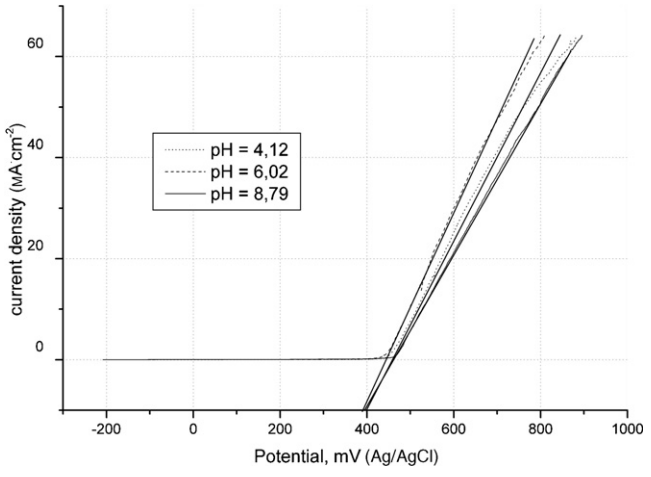

Fig. 2. LV curves for reactor-grade U metal in 0.1 M $NaClO_4$ solution at different pH. $S = 0.03\ cm^2$, $T = 22°C$; potential scan rate = 0.2 mV min^{-1}.

Zr and Ru alloy additions decrease the transpassivation potential slightly in comparison with changes in the $E_{tr.}$ for reactor-grade uranium metal. This decrease may be attributed to the enhanced grain-boundary absorption of H_2 on the saturated δ-phase for the U–Zr alloys and on U_2Ru for the U–Ru alloys. The most pronounced decrease of the transpassivation potential (100–150 mV in comparison with U metal) was observed for the U–1.3 at.% Zr alloy, apparently due to an alloy morphology favorable for H_2 adsorption.

3.3. Potential controlled electrolysis

Corrosion rates of U metal, U–1.3 at.% Zr, U–5.0 at.% Zr, and U–1.2 at.% Ru alloys in 0.1 $NaClO_4$ at pH 3.0–9.0 at ambient temperature in potential intervals around $E_{tr.}$ were determined using potential controlled electrolysis, PCE. For each measurement, the electrodes were immersed into the electrolyte with corresponding pH values. Dissolved oxygen was purged from the electrochemical cell by Ar bubbling until steady-state OCP values were achieved. The required electrolysis potential was applied to the electrode–solution interface and the *I–t* curve was measured over a period of time. The 0.1 M $NaClO_4$ solution was agitated by magnetic stirrer. Aliquots of the solution were taken regularly and the U(VI) concentration was measured spectrophotometrically with arsenazo III.

The *I–t* curves corresponding to the PCE of uranium metal, U–1.3 at.% Zr, and U–1.2 at.% Ru alloys are presented in Fig. 3. Increase of the applied potential from 300 to 500–600 mV/Ag/AgCl increased the observed current density for all tested metals (Fig. 3A–F). For all electrodes in all investigated electrolyte pH and applied potential, the PCE measurements showed increased current with time, apparently due to increasing electrode surface area. This increase of the electrode surface may be associated with the pitting corrosion that is usually observed for uranium alloy electrodes in solutions with high oxidation potentials [17]. During pitting corrosion, the electrode oxidation is localized at the intergranular interface and causes spallation of the alloy particles and oxidation products from the electrode surface. The greatest oscillations of the current were observed for the U metal electrode. Increase of electrolyte pH did not significantly affect the absolute values of the corrosion current density for the reactor-grade U metal electrode (Fig. 3A and D). At the same time, the oscillations of current densities for this electrode over time were less pronounced. This was true even at $E = 600$ mV/Ag/AgCl, significantly higher than the transpassivation potential. These observations indicate that increasing electrolyte pH leads to more uniform uranium metal corrosion.

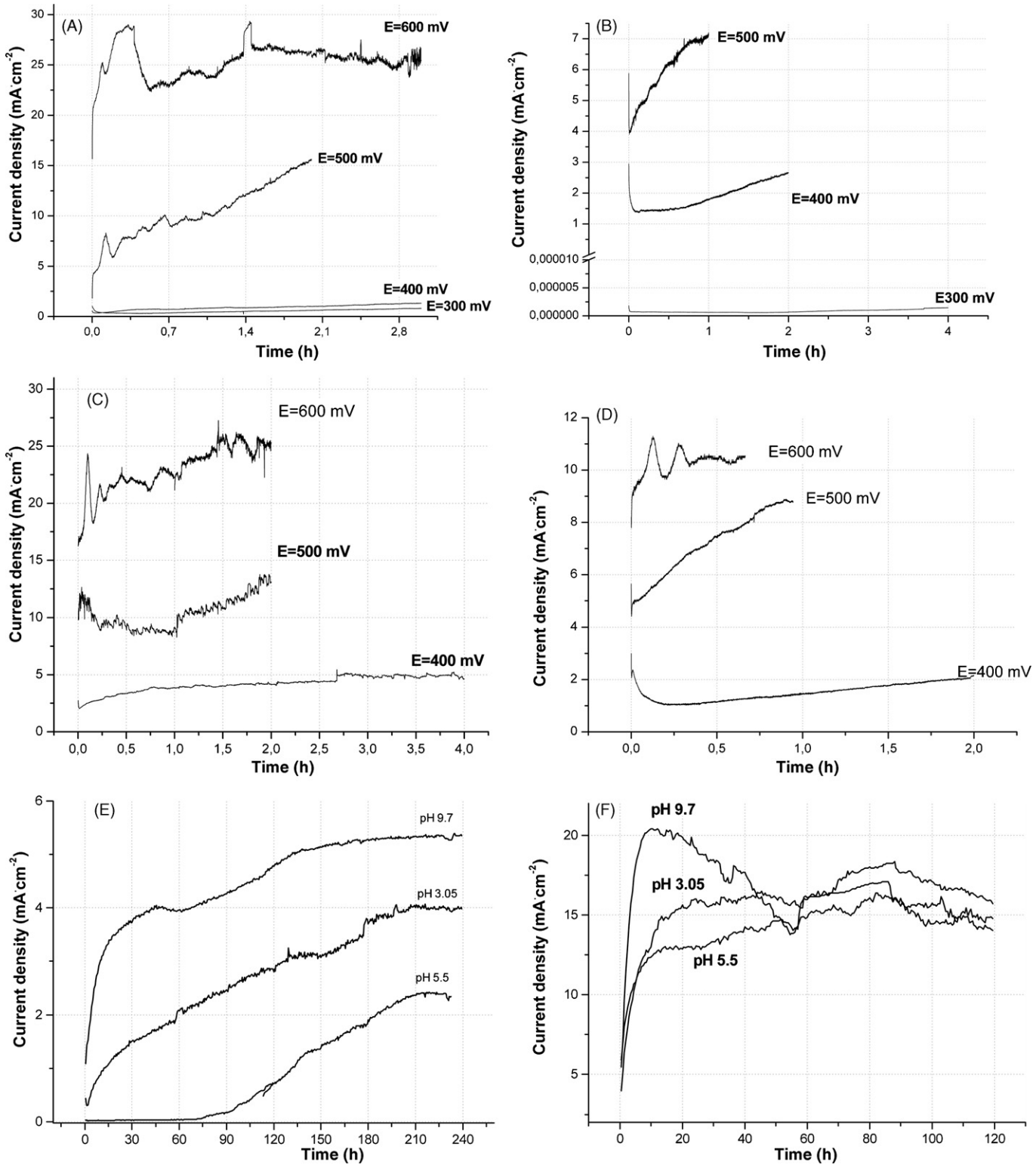

Fig. 3. *I–t* curves for PCE for U metal, U–1.3 at.% Zr, and U –1.2 at.% Ru electrodes in 0.1 M $NaClO_4$ at different pH and electrode potentials. Electrode surface = 0.16 cm^2, $V_{el.}$ = 10 ml; $T = 22 \pm 1\,^{\circ}C$. (A) U metal, pH 4.00; (B) U–1.3 at.% Zr (pH 4.0); (C) U metal, pH 9.00; (D) U–1.3 at.% Zr (pH 9.0); (E) U–1.2 at.% Ru, E = 300 mV; (F) U–1.2 at.% Ru, E = 500 mV.

The absolute values of current densities observed during PCE of U–1.3 at.% Zr and U–1.2 at.% Ru were significantly lower than for reactor-grade uranium metal (compare Fig. 3A and C with Fig. 3B and D–F). The effect of Zr alloy addition was more pronounced than that of Ru. The maximum difference in the PCE current densities between reactor-grade uranium metal and U–1.3 at.% Zr electrodes was observed at 300–400 mV/Ag/AgCl in pH 4.0 electrolyte (Fig. 3A and B).

Table 3
Rates and current efficiency of uranium metal and alloys corrosion

pH	E (mV Ag/AgCl)	U metal		U–1.3 at.% Zr		pH	U–1.2 at.% Ru	
		CR (mg cm^{-2} h^{-1})	CE (F/mol)	CR (mg cm^{-2} h^{-1})	CE (F/mol)		CR (mg cm^{-2} h^{-1})	CE (F/mol)
4.00	300	1.21	6.84	0.89	5.08	3.05	3.52	4.08
	400	2.65	7.6	3.72	4.75			
	500	12.10	7.88	12.23	4.55		21.05	4.98
	600	40.4	5.58	–	–		–	–
7.00	300	1.89	5.90	0.13	8.12	5.50	2.44	3.35
	400	6.52	5.87	2.81	4.96			
	500	13.6	7.16	16.55	4.04		26.9	5.23
	600	24.9	7.96	23.54	4.08		–	–
9.00	300	2.01	6.03	0.08	6.83	9.7	7.36	5.48
	400	7.58	6.1	2.63	7.08		–	–
	500	14.2	–	11.44	4.21		24.87	5.85

The less marked effect of Ru alloy addition, especially in pH 9.0 solution (Fig. 3C and F), may be associated with the presence of the U_2Ru phase at the electrode surface (Table 1). The presence of the intermetallic compound at the electrode surface may induce an additional galvanic potential and thus increase the anodic current density. At the same time, during PCE of the U + 1.2 at.% Ru electrode in 0.1 M $NaClO_4$ (pH 5.51), an induction period was observed during the first hour of electrolysis at $E = 300$ mV/Ag/AgCl, i.e., below the transpassivation potential of this alloy (Table 2). This observation could be associated with formation of a sparingly soluble U(IV–VI) hydroxide at the electrode surface. Apparently, the combination of electrolyte pH and the applied electrode potential corresponds to the maximum over voltage of U(IV) oxidation to more soluble species U(VI) species. Shift of the electrolyte pH to lower values (3.05) increases the solubility of U(IV), while pH increase shifts the U(IV)/U(IV) oxidation potentials negatively, leading in both cases to formation of more soluble oxidation products. Thus, the analysis of *I–t* curves measured during PCE of uranium metal, U–1.3 at.% Zr, and U–1.2 at.% Ru alloys indicates that the presence of about 1 at.% alloy addition, i.e., below the threshold alloy addition concentrations [6,14], should decrease the corrosion rate of the corresponding alloys.

During the PCE, the uranium metal and alloy electrodes were covered with black insoluble corrosion products. Some insoluble residue was also found in the electrolyte. The insoluble substance was removed from the electrode and added to the electrolyte. The solution was acidified to pH 1.0–2.0 with 11.0 M HCl and heated gently in contact with air to oxidize uranium quantitatively to UO_2^{2+}. The corrosion rates (CR) and current efficiency (CE) of PCE at different oxidation potentials and electrolyte pH were calculated based on the analyzed uranium corrosion product concentrations (Table 3).

Comparison of the data for reactor-grade U metal and for U–1.3 at.% Zr alloy in pH 4 0.1-M $NaClO_4$ solution shows, in contradiction with the data of corresponding *I–t* curves, that similar CR were observed for both electrodes. This discrepancy becomes clear after consideration of the corresponding CE values. CE values close to or greater than 6.0 F/mol observed for the U metal electrode correspond to total uranium oxidation to U(VI) due to the electrode reaction. At the same time, the lower current efficiency (4.75–5.5 F/mol) for the U–1.3 at.% Zr alloy electrode suggests that the uranium species pass to the electrolyte not only due to electrochemical reaction, but also by the spallation of U-containing species such as alloy grains or UO_{2+x}. The subsequent oxidation of the latter particles to U(VI) takes place during the electrolyte treatment but before the uranium quantitative determination. Increasing electrolyte pH increases the differences in CR values observed during PCE of U metal and U–1.3 at.% Zr electrodes at $E < 500$ mV/Ag/AgCl, as expected from analysis of the corresponding CV curves. However, increasing the applied potential to 600 mV/Ag/AgCl decreases the CE of the alloy electrode and correspondingly increases the CR (Table 3).

The effect of spallation of non-oxidized particles on the corrosion rate was found by comparing the behavior of U metal and the U–1.2 at.% Ru alloy. The data, presented in Table 3, indicate that over the studied range of electrolyte pH and applied electrolysis potentials, the calculated CR values for the alloy electrode were comparable to or greater than those obtained for pure uranium metal. It is also important to note that the CE values calculated for U–1.2 at.% Ru were 3.5–5.0 F/mol, again indicating the importance of the spallation phenomenon to the efficiency of U oxidation to U(VI).

4. Conclusions

Electrochemical study of reactor-grade uranium metal and its Zr and Ru alloys in neutral, pH 3.0–9.0, 0.1 M $NaClO_4$, electrolyte at potentials near transpassivation demonstrate that the transpassivation potentials are weakly affected by the alloy addition and electrolyte pH and are found at 400–460 mV/Ag/AgCl. The anomalous transpassivation potential for the U–1.3 at.% Zr alloy electrode seemingly is due to the effect of alloy microstructure, favoring H_2 adsorption to decrease the transpassivation potential. Analysis of the *I–t* curves, measured during PCE of uranium metal and alloy electrodes at 300–600 mV/Ag/AgCl, indicate that introduction of Zr and Ru to uranium apparently

decreases the rate of electrochemical oxidation in comparison with the corresponding rate for pure uranium metal. At the same time, the observed corrosion rates, which take into account the spallation of U metal or alloy grains and/or UO_{2+x} particles from the electrode surface during electrolysis, were found to be similar for the uranium metal and the studied alloys. Thus, the obtained results indicate that the corrosion rate of low-alloyed uranium (such as the irradiated uranium metal fuel rods in K basins) is determined not only by the concentration of the fission products, but, most probably, by their effect on the mechanical strength of the alloy and the passive film towards spallation during corrosion.

Acknowledgement

The work is supported by US DOE CRDF Grant No. RUC-2-20007-MO-04.

References

[1] J.T. Waber, A Review of the Corrosion Behavior of Uranium. Report LA-2035, Los Alamos Scientific Laboratory, NM, December 1958.
[2] W.D. Wilkinson, Uranium Metallurgy, Interscience Publishers, New York, 1962, Chapter 7.
[3] V.V. Gerasimov, Corrosion of Uranium Metal and Alloys, "Atomizdat" Publ. Co., 1965, p. 96 (in Russian).
[4] A.M. Fedosseev, A.B. Iussov, V.F. Peretrukhin, C.H. Delegard, Radiochemistry 48 (6) (2006) 513–516 (pages are indicated in Russian version of the journal).
[5] J.C.S. Dalton, J. Chem. Soc. (1973) 604–607.
[6] B.A. Hilton, Review of Oxidation Rates of DOE Spent Nuclear Fuel: Part 1: Metallic Fuel. Report ANL ANL-00/24, November 2000, p. 100.
[7] T.H. Bauer, J.K. Fink, D.P. Abraham, I. Johnson, S.G. Johnson, R.A. Wigeland, Modeling Corrosion and Constituent Release from a Metal Waste Form. Report ANL/RAE/CP-103572, January 5, 2001, p. 12.
[8] J. Fonnesbeck, Embedded Topical Meeting on DOE Spent Fuel and Fissile Material Management, San Diego, CA June 4–8, 2000.
[9] C.H. Delegard A., J. Schmidt, R.L. Sell, S.I. Sinkov, S.A. Bryan, S.R. Gano, B.M. Thornton, Final Report–Gas Generation Testing of Uranium Metal in Simulated K Basin Sludge and in Grouted Sludge Waste Forms, Report PNNL-14811, August 2004, p. 55.
[10] S. Orman, Oxidation of Uranium and Uranium Alloys, in: J.J. Burke, et al. (Eds.), Physical Metallurgy of Uranium Alloys, Brook Hill Publishing Co., Chestnut Hill, MA, 1976, pp. 815–833.
[11] M.W. Burkart, Development and Properties of Uranium-Base Alloys Corrosion Resistant in High-Temperature Water. Part III. Corrosion Mechanism of Uranium-Base Alloys in High Temperature Water. Report WAPD-127-Part III, Westinghouse Electric Corporation: Pittsburgh, PA, 1957.
[12] M.W. Burkart, B. Lustman, J. Met. 10 (26) (1958) 214–219.
[13] R.K. McGeary, Development and Properties of Uranium-Base Alloys Corrosion Resistant in High-Temperature Water. Part I. Alloys Without Protective Cladding, WAPD-127-Part IV, Westinghouse Electric Corporation, Pittsburgh, PA, 1957.
[14] J.E. Draley, S. Greenberg, W.E. Ruther, The High Temperature Aqueous Corrosion of Uranium Alloys Containing Minor Amounts of Niobium and Zirconium, ANL-5530, 1957.
[15] A.E. Dwight, M.H. Mueller, Constitution of the Uranium-Rich U-Nb and U-Nb-Zr Systems, Report ANL-5581, 1956.
[16] V.V. Gerasimov, Corrosion of Uranium and its Alloys in Aqueous Solutions, "Atomizdat" Publ., Moscow, 1965, p. 96 (in Russian).
[17] T. Mueller, M. Petec., Uranium. In: Encyclopedia of Electrochemistry of the Elements, vol. IXb, Chapter IXb-5, 1974.
[18] P.R. Bredt, C.D. Carlson, C.H. Delegard, K.H. Pool, A.J. Schmidt, D.B. Bechtold, J. Bourges, D.A. Dodd, T.A. Flament, N.N. Krot, A.B. Yusov, Proceedings of the WM'00 Conference, Tucson, AZ, 2000, p. 14.
[19] G. Sattonnay, C. Ardois, C. Corbel, J.-F. Lucchini, M.-F. Barthe, F. Garrido, D. Gosset, J. Nucl. Mater. 288 (2001) 11–19.
[20] I. Harrington, A. Ruele, Uranium Production Technology, Gosatomizdat Publ. Co., Moscow, 1961 (Russian version).
[21] The Analytical Chemistry of Zirconium, in: The Analytical Chemistry of the Elements Series, "Nauka" Publ., 1966, p. 221 (in Russian).
[22] The Analytical Chemistry of Platinum Group Metals, in: The Analytical Chemistry of the Elements Series, "Nauka" Publ., 1966, p. 345 (in Russian).
[23] A.A. Abou-Zahra, F.H. Hammad, P. Boudeau, J. Nucl. Mater. 60 (1976) 66–78.
[24] O.S. Ivanov, T.A. Badaeva, R.M. Sofronov, V.B. Kishinevsky, N.P. Koushnir, Phase Diagrams and Transformations of Uranium Alloys, "Nauka" Publ., Moscow, 1972, p. 254 (in Russian).